Sequence-specific recognition of the internalization motif of the Alzheimer's amyloid precursor protein by the X11 PTB domain

Zhongtao Zhang, Chi-Hon Lee[1], Valsan Mandiyan, Jean-Paul Borg[2], Benjamin Margolis[2], Joseph Schlessinger and John Kuriyan[1,3,4]

Department of Pharmacology, New York University Medical Center, 550 First Avenue, New York, NY 10016, [1]Laboratories of Molecular Biophysics, [3]Howard Hughes Medical Institute, The Rockefeller University, 1230 York Avenue, New York, NY 10021 and [2]Howard Hughes Medical Institute, Department of Internal Medicine and Biological Chemistry, University of Michigan Medical School, Ann Arbor, MI 48109, USA

[4]Corresponding author

Z.Zhang and C.-H.Lee contributed equally to this work

The crystal structure of the phosphotyrosine-binding domain (PTB) of the X11 protein has been determined, in complex with unphosphorylated peptides corresponding to a region of β-amyloid precursor protein (βAPP) that is required for receptor internalization. The mode of binding to X11 of the unphosphorylated peptides, which contain an NPxY motif, resembles that of phosphorylated peptides bound to the Shc and IRS-1 PTB domains. Eight peptide residues make specific contacts with the X11 PTB domain, and they collectively achieve high affinity ($K_D = 0.32 \mu M$) and specificity. These results suggest that, in contrast to the SH2 domains, the PTB domains are primarily peptide-binding domains that have, in some cases, acquired specificity for phosphorylated tyrosines.

Keywords: β-APP/NPxY motif/peptide recognition/PTB domain

Introduction

The phosphotyrosine-binding/phosphotyrosine interaction (PTB/PI) domain was first identified as the component of the adaptor protein Shc (Src homology 2/collagen homology) that binds to activated and tyrosine-phosphorylated receptors (Blaikie *et al.*, 1994; Kavanaugh and Williams, 1994; Batzer *et al.*, 1995b; Dikic *et al.*, 1995; Kavanaugh *et al.*, 1995; Pratt *et al.*, 1996; Ravichandran *et al.*, 1996). The interactions mediated by the PTB domains are critical for tyrosine phosphorylation of Shc and another adaptor protein, IRS-1 (insulin receptor substrate-1) (Isakoff *et al.*, 1996; Milia *et al.*, 1996; O'Bryan *et al.*, 1996; Ravichandran *et al.*, 1996; Sawka-Verhelle *et al.*, 1996); the phosphotyrosine-containing sequences in Shc and IRS-1 in turn serve as docking sites for other signaling molecules (Pelicci *et al.*, 1996; White, 1996). The architecture and peptide recognition mechanism of the PTB domains are distinct from those of the SH2 (Src homology 2) domains (Zhou *et al.*, 1995b). While the SH2 domains recognize the phosphotyrosine and peptide residues immediately C-terminal to it (Songyang *et al.*, 1993), the PTB domains (such as Shc and IRS-1) interact with peptide residues that are N-terminal to the phosphotyrosine. In addition, a β-turn formed by the motif NPxY* (N, Asn; P, Pro; x, any amino acid; Y*, phosphotyrosine) is critical for recognition (Batzer *et al.*, 1995b; Kavanaugh *et al.*, 1995; Zhou *et al.*, 1995c).

The three-dimensional structures of the Shc (Zhou *et al.*, 1995b) and IRS-1 PTB domains (Eck *et al.*, 1996) are very similar, although they share no significant sequence identity. Database searches for proteins homologous to the Shc PTB domain have led to the identification of a small number of novel PTB domains (Bork and Margolis, 1995). Of these, the X11 protein is a neuron-specific protein of as yet unknown function that contains two PDZ domains in addition to a PTB domain at its C-terminus (Duclos *et al.*, 1993; Borg *et al.*, 1996). The X11 protein has been found to bind to the cytoplasmic domain of the β-amyloid precursor protein (β-APP) *in vivo,* via its PTB domain *(*Borg *et al.*, 1996; McLoughlin and Miller, 1996). Although the biological consequence of this interaction is unclear at present, the X11 PTB domain and β-APP interact with each other with high affinity and high specificity (Borg *et al.*, 1996). β-APP appears to be the major ligand for the X11 PTB domain *in vivo* (Borg *et al.*, 1996). In addition, the X11 PTB domain discriminates against other potential PTB-binding proteins that contain the NPxY motif; in contrast to the Shc or the IRS-1 PTB domains, the X11 PTB domain does not interact with a number of tested growth factor receptors in either the activated or the resting states (J.-P.Borg and B.Margolis, unpublished data).

Biochemical characterization of the X11/β-APP interaction indicated that a NPTY motif located at the C-terminus of β-APP is essential for its association with the X11 PTB domain *(*Borg *et al.*, 1996). A 14 residue unphosphorylated peptide (APP peptide) encompassing the sequence QNGEYNPTYKFFEQ competes efficiently with full-length β-APP in binding to the X11 PTB domain, suggesting that this local sequence accounts for the binding. This region is also required for the internalization of β-APP, a process that leads to the degradation of β-APP and the formation of the pathological β-amyloid peptides (Aβ) (Haass *et al.*, 1993; Lai *et al.*, 1995). Most interestingly, the interaction between the X11 PTB domain and β-APP (as well as APP peptides) appears to be independent of phosphorylation *(*Borg *et al.*, 1996). A phosphorylation-independent interaction for Shc PTB (Charest *et al.*, 1966) and between β-APP and the FE65 PTB domain has also been reported (Fiore *et al.*, 1995; McLoughlin and Miller, 1996). The dispensability of phosphorylation for binding distinguishes the PTB domains from the SH2 domains, which strictly require their peptide targets to be tyrosine phosphorylated.

Table I. Binding affinities of APP peptides for X11 PTB domain

Peptide[a]	Sequence[b]	$K_D(\mu M)$[c]	(r^2)[d]	Relative affinity
14mer	QNGYENPTYKFFEQ	0.32 ± 0.03	0.981	1.0
E(−4)A	QNGY**A**NPTYKFFEQ	1.73 ± 0.14	0.993	0.19
F(+2)A	QNGYENPTYK**A**FEQ	3.44 ± 0.48	0.976	0.10
F(+3)A	QNGYENPTYKF**A**EQ	3.11 ± 0.30	0.989	0.11
E(+4)A	QNGYENPTYKFF**A**Q	0.59 ± 0.05	0.992	0.56
10mer	GYENPTYKFF	4.56 ± 0.70	0.963	0.07
10mer+P	GYENPTY*KFF	8.26 ± 1.71	0.932	0.04

[a]The 10 residue (10mer) and 14 residue (14mer) APP peptides were also used in the crystallographic study. Peptide residues are numbered as follows in the 14mer peptide, with the 10mer peptide encompassing residues −6 to +3:

```
 Q  N  G  Y  E  N  P  T  Y  K  F  F  E  Q
−8 −7 −6 −5 −4 −3 −2 −1 +0 +1 +2 +3 +4 +5
```

[b]* indicates that the tyrosine is phosphorylated.
[c]The equlibrium dissociation constants, K_D are determined by surface plasmon resonance (SPR) competition assay (see Materials and methods) and are averages of three independent experiments.
[d]r^2 is the coefficient of determinants.

In an effort to understand the interaction between the X11 PTB domain and the APP peptide we have determined the three-dimensional structure of the X11 PTB domain bound to the APP peptide and have carried out binding assays. We found that unphosphorylated APP peptides bind to the X11 PTB domain with affinities that are similar to other PTB/phosphopeptide interactions. However, the X11 PTB domain exhibits binding specificity that is distinct from those of Shc and IRS-1 PTB domains. In addition, the crystal structures of X11 PTB/APP peptide complexes reveals that the sequence specific recognition extends to peptide residues that are C-terminal to the NPxY motif. The extensive interactions between the unphosphorylated APP peptide and X11 PTB domain highlights the role of these modules as general peptide recognition domains.

Results

The binding of X11 PTB domain to APP peptide

Using surface plasmon resonance (SPR) analysis we found that the X11 PTB domain binds strongly to both phosphorylated and unphosphorylated APP peptides, with less than a two-fold difference in their binding affinities (Table I). The highest affinity (K_D = 0.32 μM) was observed for a 14 residue unphosphorylated APP peptide (see Materials and methods). For comparison, the K_D for the Shc PTB domain interacting with an 18 residue Trk-derived phospho-peptide is 0.04 μM (Mandiyan *et al.*, 1996) and the K_D for the IRS-1 PTB domain interacting with a 11 residue phospho-peptide corresponding to a region of the IL4 receptor is 6 μM (Zhou *et al.*, 1996). The on- and off-rates for the 14 residue unphosphorylated APP peptide were also measured, and are comparable with those of the Shc PTB/peptide interactions (Zhou *et al.*, 1995a; Laminet *et al.*, 1996). The measured dissociation rate constant (k_{off}) is 2.75×10^{-2} s^{-1} and the derived association rate constant (k_{on}) is 8.5×10^4 M^{-1}s^{-1}. The dissociation and association rate constants are ~10-fold lower than those for high affinity SH2-peptide interactions

($k_{on,}$ 1×10^5 to 2×10^6 M^{-1}s^{-1} and k_{off}, ~0.1 s^{-1}) (Panayotou *et al.*, 1993; Ladbury *et al.*, 1995).

Overall structure and peptide binding mode

The structures of two complexes of the X11 PTB domain and two peptides (10 and 14 residues long, respectively) from the APP cytoplasmic region have been determined to nominal resolutions of 2.3 and 2.5 Å, respectively. Multiwavelength anomalous diffraction (MAD) experiments (Hendrickson, 1991) were used to provide independent phase information. Crystals of X11 complexed to either peptide are in the tetragonal space group (P4$_1$2$_1$2), with cell dimensions of a = 74.4/74.6 Å and c = 157.1/155.4 Å, for the 10/14 residue peptides, respectively. The R-values are 21.2% (free R = 30.3%) and 21.0% (30.3%) for 10 residue and 14 residue peptide complexes, respectively. With respect to the tyrosine residue of the NPxY motif, which is denoted residue +0, the short peptide runs from −6 to +3, while the long peptide runs from −8 to +3 (residues +4 and +5 are disordered). Due to the higher resolution of the structure of the 10 residue peptide complex, the analysis is based mainly on that structure. There are two crystallographically independent X11/APP peptide complexes in the asymmetric unit and they are very similar (r.m.s. deviation of 0.94 Å for all Cα atoms), except for certain loops. However, there are subtle differences in terms of the detailed peptide interactions between these two complexes, indicating a certain degree of flexibility in the interface (see below).

Like the Shc and the IRS-1 PTB domains, the X11 PTB domain contains a 'PH-fold' first seen in the pleckstrin homology domain (Macias *et al.*, 1994). The PH fold consists of a central β-sandwich structure and a C-terminal α-helix (α2; Figure 1A) (Lemmon *et al.*, 1996). In X11, as in Shc (Zhou *et al.*, 1995b), a large insertion between two strands (β1 and β2) results in the formation of an additional strand (β1′) and an α helix (α1). This insertion, which is not seen in the IRS-1 PTB domain, plays a role in recognition of the peptide ligand. While the β1′ strand forms part of the β-sandwich on the edge that is opposite to the peptide binding site, the α1 helix packs against one face of the β-sheets. The N-terminal tip of helix α1 together with the β1′/α1 loop flank the bound peptide on one side, with helix α2 on the other side. The X11 PTB domain contains a unique insertion of 20 residues in the β6/β7 loop with respect to Shc. This large loop is located near the tyrosine residue of the NPxY motif of the peptide ligand (Figure 1A). However, it mediates few interactions with the bound peptide and is mostly disordered in the structure.

The APP peptide binds to the X11 PTB domain by forming an anti-parallel hydrogen bonding interaction with strand β5 of the PTB domain, thus becoming incorporated into the β-sandwich that is the structural core of the domain (Figures 1A and 3). Five peptide residues (residues −3 to −7, see Figure 3 for the numbering of peptide residues) N-terminal to the NPxY motif are involved in the antiparallel β-strand interaction. The NPTY motif of the bound peptide adopts a β-turn conformation, capping the β-strand of the peptide (Figure 1B). The peptide lies alongside helix α2 in an antiparallel orientation, and the peptide binding mode in X11 is similar to that seen in the Shc and the IRS-1 structures (Zhou *et al.*, 1995b; Eck *et al.*,
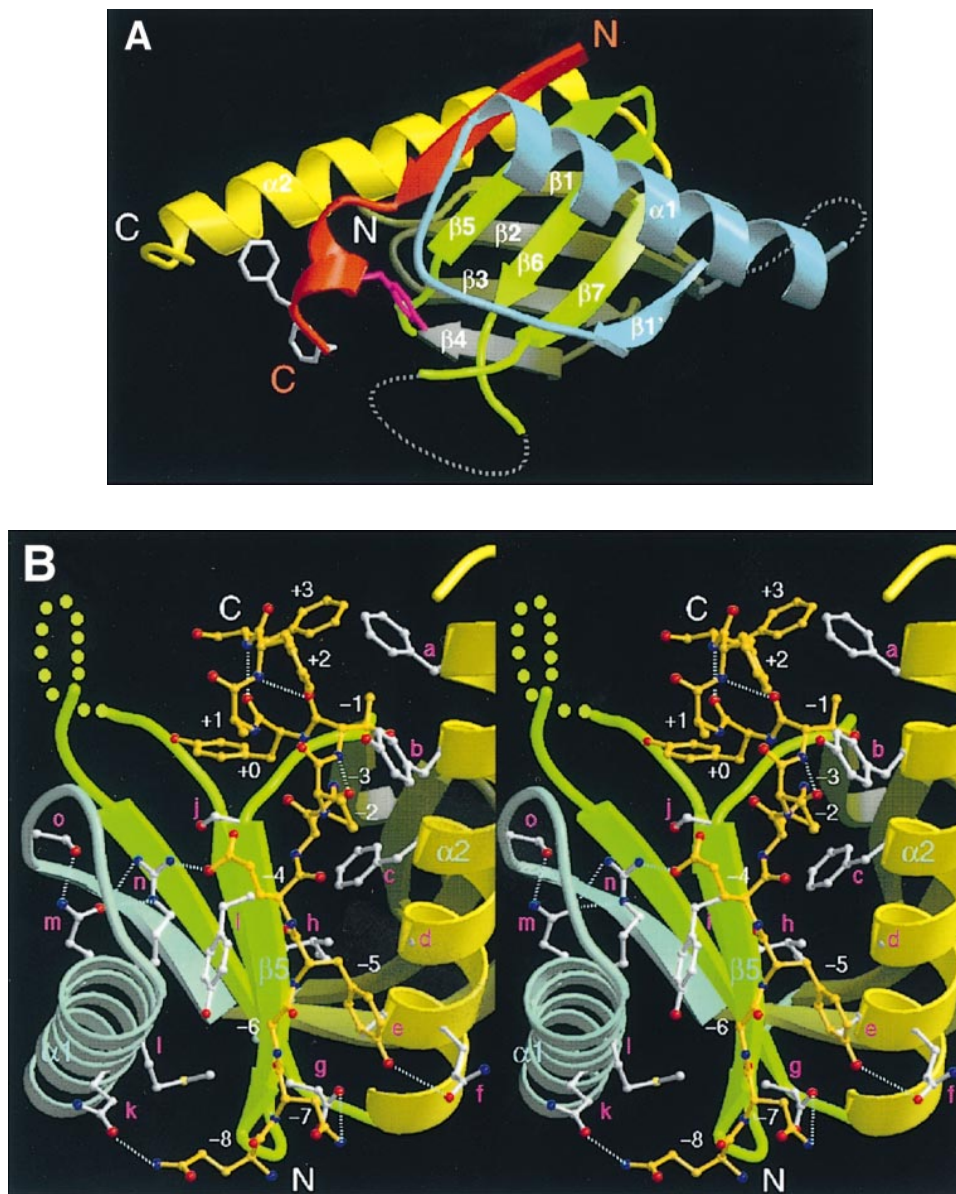
Fig. 1. (**A**) Ribbon representation of the structure of the X11 PTB domain in complex with the 14 residue APP peptide. The core structure of the X11 PTB domain resembles the 'PH' fold that consists of a β-sandwich (colored in light and dark green) and the C-terminal helix (α2; in yellow). With respect to the PH fold and the IRS-1 PTB domains, X11 PTB domain contains a insertion that forms helix α1 and strand β1′ (colored in blue). The APP peptide (colored in orange) forms an anti-parallel β-strand with the β5 strand of the X11 PTB. Also shown are the sidechains of the tyrosine (+0; in pink) and the two C-terminal phenylalalines (+2 and +3; in white) of the peptide. Residues +4 and +5 of the peptide are disordered and not shown. Two missing loops (α1-β2 and β6-β7) are indicated by dashed lines. (**B**) Stereodiagram of the interactions between the X11 PTB domain and the APP peptide. The X11 PTB domain is in a ribbon-representation, with sidechains colored in white. The peptide is shown in ball-and-stick representation with carbons, oxygens and nitrogens coloured yellow, red and blue. Sidechains of the PTB domain are labelled as follows: a, Phe486; b, Tyr483; c, Phe479; d, Gly476; e, Ala472; f, Gln473; g, Asp421; h, Ile419; i, Tyr418; j, Ser417; k, Gln358; l, Met354; m, Gln356; n, Arg353; o, Ser344. The sidechain of Lys(+1) of the peptide is removed for clarity. Figures are generated using MOLSCRIPT (Kraulis, 1991) and Raster3D (Bacon and Anderson, 1988).

1996). Upon aligning the structures of the X11 with the IRS-1 and Shc PTB domains (excluding the peptide from the calculation), peptide residues containing the NPxY motif and the residues N-terminal to it are essentially superimposable (r.m.s. deviation 1.5/1.9 Å for the peptide backbone of Shc/IRS-1 complexes, respectively). However, a unique aspect of the X11-peptide interaction is the formation of a 3^{10} helix by the C-terminal residues of the peptide, with additional interactions with the PTB domain (discussed below).

Interactions with the NPxY motif

High-affinity peptides for PTB domains typically contain an NPxY motif (usually phosphorylated on tyrosine) (Zhou *et al.*, 1995c) that has been shown to adopt a β-turn conformation in solution even in the absence of the PTB domains (Trub *et al.*, 1995). In the three currently available PTB structures (Shc, IRS-1, and X11), the NPxY motif (phosphorylated in Shc and IRS-1, unphosphorylated in X11) adopts a type I β-turn conformation when bound to the PTB domains. The Asn residue of the -3 position of

the NPxY motif has a conserved structural role for stabilizing the β-turn conformation (Zhou *et al.*, 1995b; Eck *et al.*, 1996). The carboxamide oxygen of the Asn(−3) sidechain forms an intramolecular hydrogen bond with the backbone amide group of the peptide residue at the -1 position (Figure 3). The amino group of the Asn sidechain is hydrogen bonded to the carbonyl groups of Leu413 and Ile416 of the X11 PTB domain. Asn(−3), and hence the β-turn conformation, appears to be the most important determinant for interaction with the PTB domains. A similar hydrogen bonding pattern was observed in the structure of the IRS-1/peptide complex (Eck *et al.*, 1996) and is expected to be conserved in other PTB/ NPxY peptide interactions as well. Pro(−2) also plays a role in stabilizing the β-turn conformation of the peptide ligand; however, its importance varies. Replacing Pro(−2) with Ala decreases the binding affinity to the Shc PTB domain up to 50-fold, depending on the sequence contexts of the peptide (Wolf *et al.*, 1995; Laminet *et al.*, 1996; Mandiyan *et al.*, 1996). In the X11 structure, the pyrrolidine ring of Pro(−2) packs against the aromatic ring of Tyr483 (from helix α2; Figures 1B and 3) while similar hydrophobic interactions are provided by the aliphatic portion of the Arg258 sidechain in the IRS-1 PTB domain (Eck *et al.*, 1996).

In the X11/APP peptide structure, the peptide is unphosphorylated. Despite the lack of a phosphate group, Tyr(+0) at the tip of the β-turn assumes a conformation that is almost identical to that of the bound phosphotyrosine residue observed in the IRS-1 and the Shc structures. As in Shc (Zhou *et al.*, 1995b), the aromatic ring of Tyr(+0) forms hydrophobic interactions with the Cβ atom of Ser417 (Figures 1B and 3), while similar interactions are mediated by Arg212 in the IRS-1/peptide structure (Eck *et al.*, 1996). Apart from this, no other specific interactions for this tyrosine residue are observed. In particular, positively charged residues (Lys346, Arg431, Arg432, Arg433 and Arg353) in the general vicinity of the tyrosine hydroxyl group are mostly disordered in the structure (Figure 5A). Interestingly, Tyr(+0) is not critical for the recognition of the peptide, since replacing this residue with Ala results in no significant loss of binding affinity (Borg *et al.*, 1996).

The C-terminal specificity

In general, the peptide residues N-terminal to the NPxY motif are considered to be the primary determinants of the binding specificity of the PTB domains (Zhou *et al.*, 1995b, 1996; Eck *et al.*, 1996). However, in X11 the C-terminal residues (Phe +2 and +3) of the APP peptide contribute positively to binding affinity. Mutation of either Phe +2 or +3 to Ala separately decreases the binding affinity by 10-fold (Table I). Residues +1 to +3 are in a 3^10 helical conformation and the aromatic rings of Phe +2 and +3 of the APP peptide pack against a hydrophobic surface that is formed by a number of residues contributed by helix α2 (Figures 1B and 5A). This helix is longer by three turns with respect to Shc. As a result of these additional interactions, the total surface area that is buried between the APP peptide and the X11 PTB domain is ~2000 Å², which is somewhat larger than those for Shc and IRS-1 structures (~1800 and ~1300 Å², respectively).
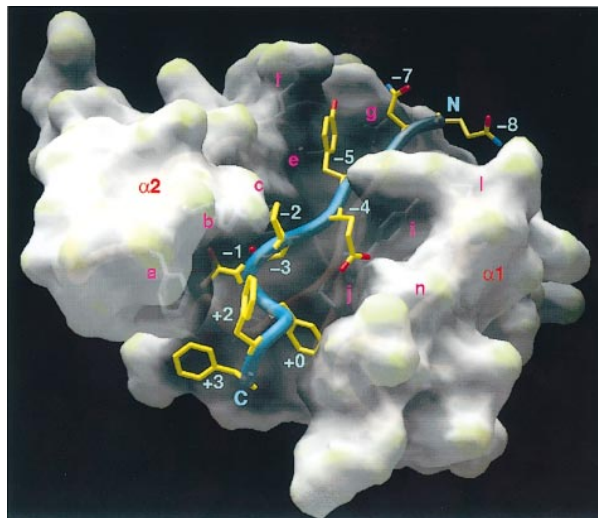
Fig. 2. Molecular surface of the X11/APP peptide complex, calculated with the peptide removed and displayed using GRASP (Nicholls *et al.*, 1991). The surface is colored according to the surface curvature calculated in the absence of peptide. The peptide (backbone shown as a blue tube) binds to a deep groove on the surface of the PTB domain. Important sidechains in the X11 PTB domain are labeled as in Figure 1B.

The N-terminal specificity

The APP peptide fits snugly into a groove on the peptide binding surface of the X11 PTB domain (Figure 2). The floor of the groove is formed by strand β5, which is part of the β-sandwich and engages in antiparallel hydrogen bonding interactions with peptide residues −4 to −8. Alternate sidechains of the peptide [Asn(−3), Tyr(−5), and Asn(−7)] interact with helix α2 (Figures 1B and 2). The other sidechains [Glu(−4), Gly(−6) and Gln(−8)] point toward strand β5 and helix α1. Two residues [Asn(−7) and Gln(−8)] of the APP peptide appear to be important for optimal binding, since removal of these two residues decreases the binding affinity by >10-fold (as judged by comparing the affinities of 14 residue and 10 residue APP peptides). In addition to the backbone hydrogen bonding, the sidechain of Asn(−7) also forms hydrogen bonds with the sidechains of Asp 421 and Gln 469 (of X11) (Figure 1B). The polar nature of the peptide residue at position −7 in APP peptide is in contrast to high affinity peptides for Shc and IRS-1, which tend to contain hydrophobic residues at this position (Wolf *et al.*, 1995).

The X11 PTB domain also has selectivity for two other peptide residues: Tyr(−5) and Glu(−4). Mutation of Tyr(−5) to Gly abolishes the binding of APP to X11 (Borg *et al.*, 1996). The aromatic ring of Tyr(−5) packs against the Cα atom of Gly476 and the sidechains of Ala472 and Ile419 (of X11) (Figures 1B and 2). The hydrophobic nature of the Tyr(−5)-binding site suggests that the X11 PTB domain might select for large hydrophobic amino acid at position −5. Such a preference has been described for the Shc PTB domain (Trub *et al.*, 1995; Laminet *et al.*, 1996; van der Geer *et al.*, 1996). Hydrogen bonding between the hydroxyl group of the Tyr(−5) and the sidechain of Gln473 (of X11) was observed in one of the two complexes in the asymmetric unit of the crystal (but not in the other complex), implying that this interaction is dispensable.
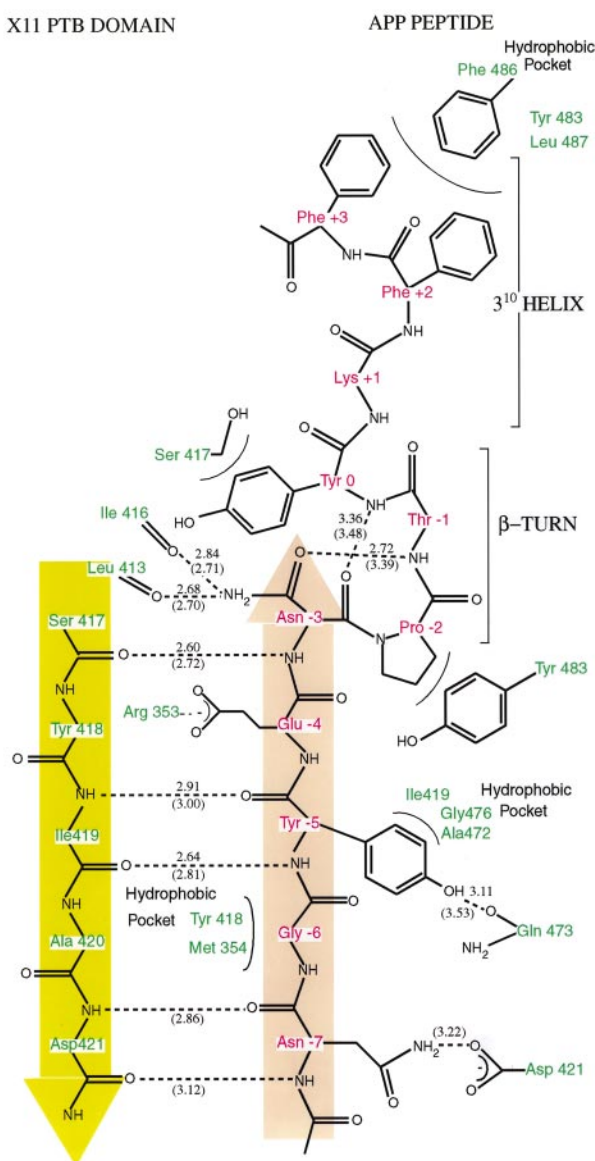
Fig. 3. Schematic depiction of contacts between the APP peptide and the X11 PTB domain. The β strands are shaded green and orange for the PTB domain and the peptide, respectively. Hydrogen bonds are shown as dotted lines, and the distance between the atom attached to the donor hydrogen and the acceptor is shown (in Å) for the 10-residue (above the lines) and the 14-residue (in parentheses, below the lines) peptide complexes.

Replacing Glu(–4) with Ala reduces binding affinity by 5-fold (Table I). In the structure, the Glu(–4) sidechain forms a salt bridge with Arg353 (of X11) which in turn is held in position by hydrogen bonds with sidechains of Gln356 and Ser344 (of X11) (Figure 1B). Arg353 is mostly buried upon ligand binding. Selectivity for an acidic residue at position –4 has been described for the Shc PTB domain also (Laminet *et al.*, 1996). Finally, the selectivity for a glycine at position –6 is suggested by the present structure. Met354 and Tyr418 (of X11) form hydrophobic interactions with the Cα atom of Gly(–6) (Figures 1B and 2). Given these steric constraints, this position is expected to accommodate only small hydrophobic residues.

Discussion

The discovery of PTB domains originated from their ability to bind to phosphorylated tyrosine residues in signaling proteins, but with sequence specificity that is fundamentally distinct from that of the SH2 domains (Kavanaugh and Williams, 1994). Subsequent structural analyses of phospho-peptide complexes of the Shc (Zhou *et al.*, 1995b) and IRS-1 (Zhou *et al.*, 1996) PTB domains showed that the architecture of these domains is related to that of the PH domains, but not to that of SH2 domains. Significantly, the recognition of phosphotyrosine residues by PTB domains relies on basic residues in the domain that are not conserved (Figure 4). The binding site for the phosphotyrosine residue lies on the edge of the domain, and the positively charged sidechains that interact with the phosphate group are exposed to solvent (Zhou *et al.*, 1995b, 1996; Eck *et al.*, 1996) (Figure 5A).

In this study we show that the recognition of the unphosphorylated form of the APP peptide by the X11 PTB domain occurs by a mechanism that is essentially the same as that utilized by the Shc and IRS-1 PTB domains to bind to phosphorylated targets. The critical elements of the recognition are the β-turn formed by the NPxY motif and the incorporation of the peptide into a β-sheet of the PTB domain. A striking feature of the X11/APP peptide complex is that the unphosphorylated tyrosine residue of the NPxY motif is bound in virtually the same conformation as is seen for the corresponding phosphotyrosine residue in Shc and IRS-1.

Quantitative binding studies demonstrate that addition of a phosphate group to the tyrosine residue of the APP peptide does not significantly change the binding affinity for the X11 PTB domain (Table I). Several charged residues that are in the vicinity of the tyrosine hydroxyl group are potentially available to coordinate the phosphate group in the phosphorylated form of APP (Figure 5A), but clearly they do so with no net stabilization of the complex. This is in contrast to the situation for Shc and IRS-1, each of which also has a constellation of positively charged residues at the phosphotyrosine-binding site. Shc and IRS-1, however, have been shown to clearly discriminate between phosphorylated and unphosphorylated targets (Zhou *et al.*, 1995b, 1996). It thus appears that different PTB domains have evolved different requirements for phosphorylation of the tyrosine of the NPxY motif in their targets.

The binding specificity of well characterized SH2 domains, on the other hand, appears to be restricted quite sharply to phosphorylated peptides. In contrast to the PTB domains, which bind tightly to their peptide targets by extensive hydrogen bonding and packing interactions, the SH2 domains have relatively limited interactions with their target peptides (Kuriyan and Cowburn, 1997). Consequently, the phosphotyrosine residue provides the major anchor point for the peptide to the SH2 domain. A comparison of the phosphotyrosine-binding sites of PTB and SH2 domains is revealing in terms of suggesting why phosphorylation of the target is dispensable in the case of certain PTB domains, but is required in the case of the SH2 domains. In the SH2 domains, a strictly conserved residue Arg175 (βB5 in the SH2 notation) rises up from the interior of the domain into a position where it can
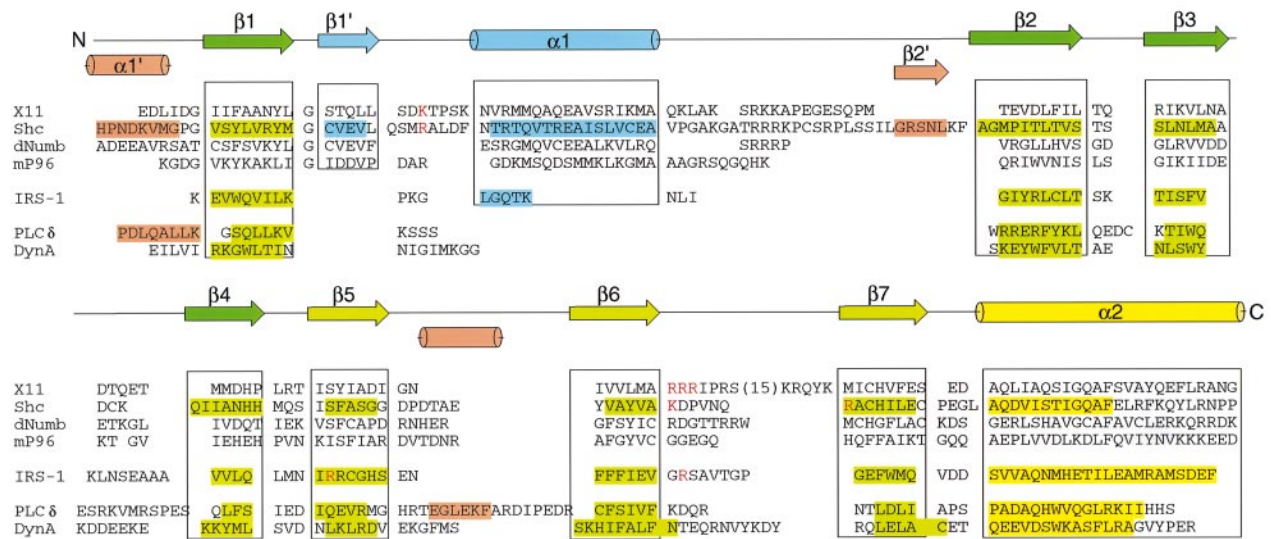
Fig. 4. Sequence alignment of PTB and PH domains. The secondary structure elements of the X11 PTB domain (residues 324 to 491) are boxed and are shown schematically as colored arrows (for β-strand) and cylinders (for α-helix) above the sequence. The secondary structure elements for Shc (Zhou *et al.*, 1995b), IRS-1 (Eck *et al.*, 1996) and two PH domains (Macias *et al.*, 1994; Lemmon *et al.*, 1996) are indicated in color. The basic residues in the vicinity of tyrosine +0 of the peptide in X11 as well as those residues in IRS-1 and Shc that coordinate the phosphotyrosine are colored red.
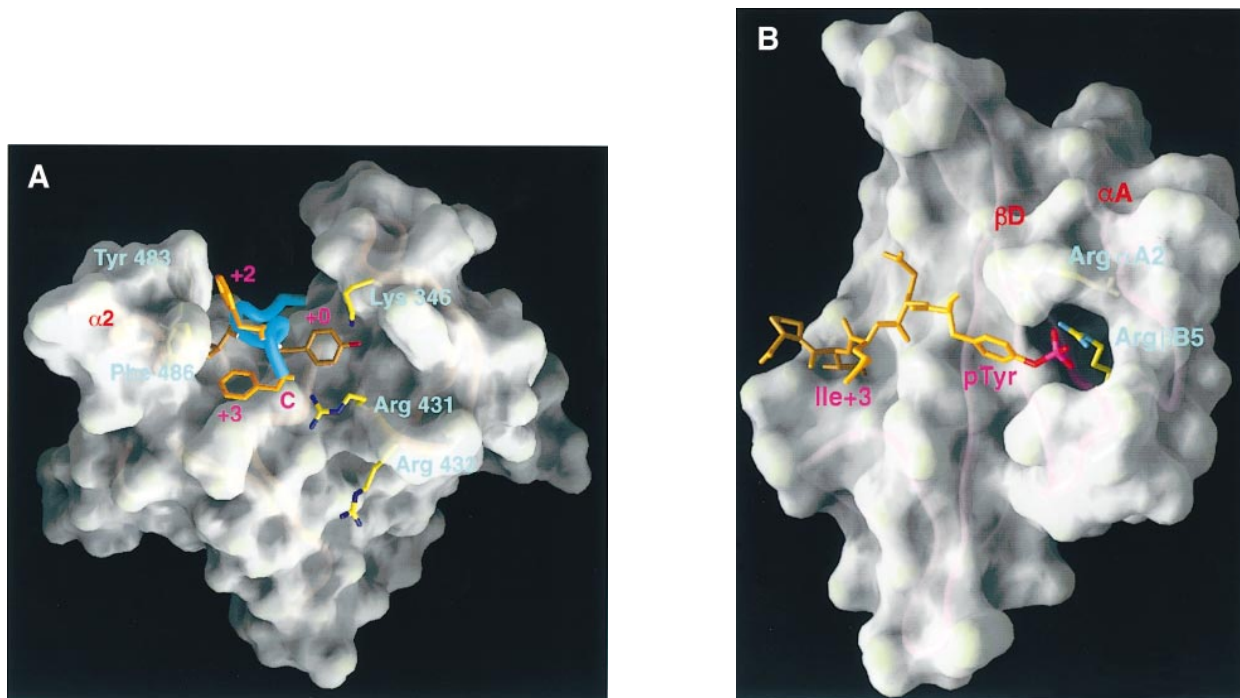
Fig. 5. Comparison of phosphotyrosine/tyrosine-binding sites of the X11 PTB domain and the Src SH2 domain. (**A**) Molecular surface of the X11 PTB domain, showing the binding site for the tyrosine (+0) and the C-terminal region of the peptide. The polypeptide backbones of the bound peptide and the X11 PTB domain are shown in red and blue tubes, respectively. Also shown are three basic residues (Lys 346, Arg431 and Arg432; removed from surface calculation) of the X11 PTB domain that are potentially involved in phosphotyrosine-binding. The sidechains of Phe(+2) and Phe(+3) of the peptide (colored in yellow) pack against the sidechains of Tyr483 and Phe 486 of the X11 PTB domain (colored in gold). (**B**) Molecular surface of an unliganded Src SH2 domain (Waksman *et al.*, 1993) showing the deeply buried ArgβB5 sidechain (not included in surface calculation). For reference, the structure of a high affinity phosphopeptide is also shown (colored in gold), taken from the pYEEI/Src complex (Waksman *et al.*, 1993). The polypeptide backbone of the Src SH2 domain is shown in purple tubes.

engage two oxygens of the phosphate group of the ligand (Figure 5B). This sidechain is quite buried in the SH2 structures. For example, in the uncomplexed Src SH2 structure (Waksman *et al.*, 1993), the total surface accessibility for ArgβB5 ranges from 2 to 6 Å² for the four molecules in the crystallographic asymmetric unit (Figure 5B). This may be compared with a surface accessibility of ~100 Å² for Arg155 (αA2), an SH2 residue that engages the phosphotyrosine from the surface. Analysis of the structures of other uncomplexed SH2 domains, such as

that of Syp/SH-PTP2 (Lee *et al.*, 1994), reveals that the buried nature of ArgβB5 is a conserved feature of the SH2 architecture (the solvent accessible surface for ArgβB5 is ~11 Å^2 in SH-PTP2).

The burial of ArgβB5 in the SH2 structure, with limited hydrogen bonding partners, is likely to have a significant energetic penalty (Honig and Nicholls, 1995) and is probably a critical architectural feature that then demands that the ligand be phosphorylated in order to neutralize the residue. In X11, basic residues that are in a position to potentially interact with the phosphate group of phosphorylated ligands are all on the surface, and the lack of stabilization of phosphorylated versus non-phosphorylated APP peptide is likely to be a consequence of an unfavorable desolvation energy for these sidechains. However, the situation for PTB domains is clearly subtle, since the Shc and IRS-1 PTB domains do bind much more strongly to phosphorylated peptides than they do to nonphosphorylated ones (Kavanaugh and Williams, 1994; Batzer *et al.*, 1995b; Trub *et al.*, 1995; Wolf *et al.*, 1995). As in X11, in the Shc and IRS-1 PTB the charged sidechains that interact with the phosphotyrosine are solvent-accessible and on the surface. The net stabilization of phosphorylated peptides in this case must be the result of particularly favorable geometries of interaction, an issue that will be of interest to investigate further.

Sequence-specific recognition of peptides by the X11 PTB domain involves a number of residues distributed over a relatively long region (10 to 13 residues) of the peptide ligands. The differences in binding specificity between X11 and the other characterized PTB domains indicate that the PTB domains are capable of mediating a broad spectrum of sequence-specific interactions. In particular, our finding that C-terminal specificity can also be a feature of PTB interactions further extends the specificity of the PTB domain. Thus, the overlapping specificity between Shc and IRS-1 PTB domains likely reflects their shared biological functions in targeting common growth factor receptors instead of a limited repertoire of the PTB-mediated interactions.

The understanding of the biological function of the X11/β-APP interaction has been impeded by our limited knowledge of these two proteins. While β-APP appears to play a role in learning processes through an unknown mechanism (Muller *et al.*, 1994), there has been no known function assigned to X11. However, the measured high specificity and high affinity as well as the conserved peptide binding mode observed in the X11/APP peptide structure suggests that the interaction might be relevant. Moreover, elimination of the X11 PTB domain binding site (sequence YENPTY) on APP severely diminished APP internalization and decreased the production of amyloidogenic Aβ peptide (Koo and Squazzo, 1994). The PTB domain of X11 appears to be solely responsible for its interaction with β-APP, since no enhanced or cooperative binding to β-APP was observed for the full-length X11 protein (J.-P.Borg and B.Margolis, unpublished data). The present study reveals the critical determinants for X11/β-APP interactions. Such information should facilitate further dissection of physiological functions of β-APP as well as the pathology of Alzheimer's disease.

Materials and methods

Protein expression and purification

The X11 PTB domain (residues 324–504) was amplified from a human fetal brain cDNA library (Stratagene) by PCR. The amplified fragment was cloned into a PET3a vector so that the gene for the PTB domain was under the control of a T7 promoter. The complete DNA sequence of the X11 PTB domain was confirmed by dideoxy sequencing. The X11 PTB domain protein was expressed in *Escherichia coli* (BL21 strain) and was purified by passing through a Q-Sepharose and size exclusion chromatography (yielding >50 mg of purified protein per liter of cell culture). Se-methionine (Se-Met)-labeled protein was expressed (Hendrickson *et al.*, 1990) and purified using similar procedures as for the native protein. The identity of the protein was confirmed by N-terminal amino acid sequencing and mass spectroscopic analysis.

An Fmoc-based strategy in conjunction with standard side chain protecting groups was applied for peptide synthesis. Fmoc-L-tyrosine (PO$_3$H$_2$)-OH was used for incorporation of phosphotyrosine (Batzer *et al.*, 1995a). Peptides were purified by ether precipitation and reverse phase HPLC.

Peptide binding studies

Surface plasmon resonance (SPR) measurements were carried out on a BIAcore Biosensor instrument (BIAcore 1000, Pharmacia Biosensor). The wild-type APP 14 residue peptide was cross-linked to a CM5 sensor chip by the amine coupling method (Felder *et al.*, 1993). Various concentrations (0.1–10 μM) of the X11 PTB domain were injected onto the cross-linked surface and the association and dissociation responses were followed. The same concentrations of the protein were also injected onto a non-cross-linked surface to measure the background signals, which were then subtracted from the binding responses. All binding experiments were performed at 25°C with a flow rate of 10 μl/min in HBS buffer (10 mM Hepes, pH 7.4, 150 mM NaCl, 1 mM EDTA, 0.05% surfactant P20 and 1 mM DTT). The binding properties of various mutant and phosphorylated peptides were followed by competition experiments. Here, various concentrations of peptides were pre-mixed with a given concentration of PTB domain protein and their binding responses to the cross-linked surface were evaluated. All data obtained were the average of at least four independent experiments. The kinetic parameters were evaluated using the BIAevaluation software (Pharmacia).

Crystallization and data collection

The X11 PTB domain protein was mixed with excess peptide (peptide:protein ratio of 1.5 or greater) in 10 mM Hepes (pH 7.5), 150 mM NaCl, and 1 mM DTT. Crystallization conditions were scanned using the hanging-drop method. Crystals of the complex were obtained in several days at 21°C with ammonium sulfate as the precipitant (1.4 M ammonium sulfate, pH 6.5, 100 mM MES, 100 mM NaCl, for the 10-residue peptide complex; and 1.8 M ammonium sulfate, pH 6.5, 100 mM Mes, for the 14-residue peptide complex). The crystals belong to the tetragonal space group (P4$_1$2$_1$2, $a = b = 74.4/74.6$ Å, $c = 157.1/155.4$ Å for the 10/14 residue peptide complexes, respectively) and diffract to beyond 2.5 Å using an in-house X-ray source. Crystals of the Se-Met labeled protein diffract X-rays more strongly than those of native protein, and the Se-Met crystals were used for all the structural analysis.

All diffraction data were collected from crystals cooled to 100 K after cryoprotection in 5–30% glycerol. X-ray data for MIR analysis were collected on a Rigaku RAXIS IIC area detector mounted on a Rigaku RU200 X-ray generator (Molecular Structure Corporation, USA). Crystals were derivatized before data collection by soaking in 15 mM trimethyl lead acetate for 24–36 h. MAD data were collected from a single frozen crystal (10 residue peptide complex; Se-Met derivative) at the National Synchrotron Light Source (Brookhaven Nation Laboratory) using beamline ×25. All data were processed using program DENZO and SCALEPACK (Z.Otwinowski and W.Minor).

Phase determination

Crystals of the 10 residue peptide complex soaked in solutions containing 15 mM trimethyl lead acetate yielded a derivative and still retained high resolution diffraction (2.5 Å). The positions of two bound lead atoms were determined using the program SHELX-90 (Sheldrick, 1991). Heavy atom parameters were then refined and initial phases were calculated for two alternative space groups (P4$_1$2$_1$2 and P4$_3$2$_1$2) in combination with two different heavy atom configurations, using the program MLPHARE (Z.Otwinowski, unpublished program). The resulting SIRAS maps were

Table II. Data collection and refinement statistics

Crystallographic analysis statistics: (for X11/10mer peptide complex)

Data set	Resolution (Å)	Reflections measured/unique	Completeness(%) overall/outer shell	Rmerge(%)[a] overall/outer shell	Riso[b]	Phasing power
SIRAS analysis						
Se-Met	30–2.5	70368/15538	97.0/95.6	6.9/27.0		
(Seleno-methionine, in-house X-ray source)						
MePbAc	30–2.5	113378/16169	99.8/98.7	8.3/34.7	0.22	0.88
(trimethyl lead acetate, 2 sites, in-house X-ray source)						
	Overall SIRAS figure of merit 0.32 (20~2.7Å)					
MAD analysis						
Se-Met (13 sites, BNL synchrotron, Beamline X25)						
λ1(0.9770Å)	30.0–2.6	117094/14337	99.6/97.4	8.3/26.6 (14.4 at 2.9Å)	0.0453	
λ2(0.9793Å)	30.0–2.6	118270/14300	99.9/99.6	8.8/30.2 (15.6 at 2.9Å)	0.0349	
λ3(0.9797Å)	30.0–2.6	118133/14326	99.3/94.3	8.5/27.6 (14.5 at 2.9Å)	–	
	Overall MAD figure of merit 0.66 (15~2.9Å)					
Data sets used for refinements						
X-11/10mer peptide (in-house X-ray source)						
Se-Met	30–2.3	69525/18927	92.4/80.0	8.3/22.9		
X-11/14mer peptide (in-house X-ray source)						
Se-Met	30–2.4	97157/17790	99.3/99.2	5.4/30.2		

Refinement statistics

	X11/APP peptide(14mer)	X11/APP peptide (10mer)
Resolution (Å)	6.0–2.5	6.0–2.3
Completeness (%) ($|F|>2.0\ \sigma|F|$)	82.7	69.0
R-factor (Free R[c]) (%)	21.2 (30.3)	21.0 (30.3)
Completeness (%) ($|F|>0\ \sigma|F|$)	93.4	91.3
R-factor (Free R)[c,d] (%)	23.2 (32.5)	24.5 (34.4)
Number of non-hydrogen atoms	2221	2155
Number of residues	285 (390)	266 (384)
Number of waters	161	215
R.m.s.d. bond lengths (Å)	0.010	0.010
R.m.s.d. bond angles (Å)	1.8	1.8
R.m.s.d. B value(bonds) (Å^2)	1.30	1.54
R.m.s.d. B value(angles) (Å^2)	1.65	1.81

[a]$R_{\mathrm{merge}} = 100 \times \Sigma_h\, \Sigma_i\, |I_{h,i} - <I_h>|\, /\Sigma_h\, \Sigma_i\, I_{h,i}$
[b]$R_{\mathrm{iso}} = \Sigma_h |F_{nat,h} - F_{deriv,h}|/\Sigma_h\, F_{nat,h}$. For MAD analysis, R_{iso} is calculated between data at two wavelengths. Wavelength 2 is used as reference data set (F_{nat}) in this calculation and F_{deriv} refers to data at another wavelength.
[c]Free R-factor was calculated using 10% of the data.
[d]Note that data with $|F| < 2\sigma|F|$ were not used in the refinement.

generally uninterpretable, consistent with the low value of figure of merits (0.32). We therefore sought additional phase information.

A multiwavelength anomalous diffraction (MAD) experiment was performed on the Se-Met derivative of the 10 residue peptide complex. For MAD data collection, a single Se-Met crystal was mounted, after flash freezing, with the c* axis approximately parallel to the spindle in order to facilitate the data collection. The inverse beam method was used to collect Bijvoet pairs of reflection. Data collection at three wavelengths near the Se absorption edge (Table II) were recorded on a Mar detector and beamline X25, National Synchrotron Light Source, and processed with DENZO and SCALEPACK. The positions of 13 Se atoms (out of a total 16 Se atoms) in the asymmetric unit were identified by difference Fourier techniques using the phases calculated from the lead derivative. Heavy atom parameters were then refined and phases were calculated using the program MLPHARE (Z.Otwinowski) for two alternative space groups ($P4_12_12$ and $P4_32_12$). Summary statistics from the MAD phasing procedure are given in Table II. Using only MAD data, phases calculated at 2.9 Å resolution with space group $P4_12_12$ yielded an interpretable electron density map which was further improved by solvent flattening and histogram matching, using SQUASH (Zhang and Main, 1990) and information from the lead derivative was not used further.

Model building and refinement
A model accounting for >90% of the structure was built into the MAD map using the program O (Jones et al., 1991) and was refined using XPLOR (Brünger, 1988) without simulated annealing. The free R value (Brünger, 1993) was used to monitor all stages of the refinement. The asymmetric unit contains two X11 PTB/APP peptide complexes which are very similar to each other. Although the noncrystallographic symmetry was not explicitly used in the refinement processes, it provided a useful check on the accurancy of the model. The resolution was later extended to 2.3 Å using a data set collected in-house. Well-ordered solvent molecules were included at this stage, and tightly restrained individual isotropic B-factors were refined.

The statistics for data collection, phase determination and refinement are given in Table II. The working R value is 21.0% using data between 6.0 to 2.3 Å and the free R value (10% of the data) is 30.3% for final model using reflections with $|F|/\sigma(|F|) > 2.0$. The current model includes two complexes of X11 PTB/APP peptide (246 residues for two X11 PTB domains and 20 residues for APP peptides), and 215 water molecules. No electron density is present for 14 residues in the α1/β2 loop, 23 residues in the β6/β7 loop and 16 residues at the C-terminus of the first X11 PTB molecule, as well as for 7 residues at the N-terminus in addition to 10 residues at the C-terminus of the second X11 PTB

molecule. The average temperature factor for protein atoms is 35.6 Å^2. Although the two X11 PTB/APP peptide complexes are very similar, certain details in the domain/peptide interfaces are slightly different (see Results).

Crystals of the X11 PTB domains in complex with the 14 residue APP peptides were also obtained, which belong to the same space group as those of X11 PTB/10 residue APP peptide complexes. The positions of two additional peptide residues at the N-terminus were identified by difference Fourier techniques using phases calculated from the model of the X11 PTB/10 residue peptide. The additional C-terminal residues are poorly ordered. A model was refined at 2.5 Å resolution using a data set collected in house. 285 residues and 161 water molecules were included in the model. The working R value is 21.2% using data between 6.0 to 2.5 Å and the free R value (10% of the data) is 30.3% for final model using reflections with $F/\sigma F > 2.0$. Both coordinate sets have been deposited in the Brookhaven Protein Data Bank with identity codes 1x11 and 1aqc for the long and short peptides, respectively.

Acknowledgements

References

Bacon,D. and Anderson,W.F. (1988) A fast algorithm for rendering space-filling molecule pictures. *J. Mol. Graphics*, **6**, 219–220.

Batzer,A.G., Blaikie,P., Nelson,K., Schlessinger,J. and Margolis,B. (1995b) The phosphotyrosine interaction domain of Shc binds an LXNPXY motif on the epidermal growth factor receptor. *Mol. Cell. Biol.*, **15**, 4403–4409.

Blaikie,P., Immanuel,D., Wu,J., Li,N., Yajnik,V. and Margolis,B. (1994) A region in Shc distinct from the SH2 domain can bind tyrosine-phosphorylated growth factor receptors. *J. Biol. Chem.*, **269**, 32031–32034.

Borg,J.-P., Ooi,J., Levy,E. and Margolis,B. (1996) The phosphotyrosine interaction domains of X11 and FE65 bind to distinct sites on the YENPTY motif of amyloid precursor protein. *Mol. Cell. Biol.*, **16**, 6229–6241.

Bork,P. and Margolis,B. (1995) A phosphotyrosine interaction domain. *Cell*, **80**, 693–694

Brünger,A.T. (1988) *X-plor Manual.* Howard Hughes Medical Institute and Dept of Molecular Biophysics and Biochemistry, Yale University, New Haven, CT.

Brünger,A.T. (1993) Assessment of phase accuracy by cross validation: the free R value. Methods and applications. *Acta Crystallogr.*, **D49**, 24–36.

Charest,A., Wagner,J., Jacob,S., McGlade,C.J. and Tremblay,M.L. (1996) Phosphotyrosine-independent binding of SHC to the NPLH sequence of murine protein-tyrosine phosphatase-PEST. Evidence for extended phosphotyrosine-binding/phosphotyrosine interaction domain recognition specificity. *J. Biol. Chem.*, **271**, 8424–8429.

Dikic,I., Batzer,A.G., Blaikie,P., Obermeier,A., Ullrich,A., Schlessinger,J. and Margolis,B. (1995) Shc binding to nerve growth factor receptor is mediated by the phosphotyrosine interaction domain. *J. Biol. Chem.*, **270**, 15125–15129.

Doyle,D.A., Lee,A., Lewis,J., Kim,E., Sheng,M. and MacKinnon,R. (1996) Crystal structures of a complexed and peptide-free membrane protein-binding domain: molecular basis of peptide recognition by PDZ. *Cell*, **85**, 1067–1076.

Duclos,F., Boschert,U., Sirugo,G., Mandel,J.L., Hen,R. and Koenig,M. (1993) Gene in the region of the Friedreich ataxia locus encodes a putative transmembrane protein expressed in the nervous system. *Proc. Natl Acad. Sci. USA*, **90**, 109–113.

Eck,M.J., Dhe-Paganon,S., Trub,T., Nolte,R.T. and Shoelson,S.E. (1996) Structure of the IRS-1 PTB domain bound to the juxtamembrane region of the insulin receptor. *Cell,* **85**, 695–705.

Felder,S., Zhou,M., Hu,P., Urena,J., Ullrich,A., Chaudhuri,M., White,M., Shoelson,S.E. and Schlessinger,J. (1993). SH2 domains exhibit high-affinity binding to tyrosine-phosphorylated peptides yet also exhibit rapid dissociation and exchange. *Mol. Cell. Biol.*, **13**, 1449–1455.

Fiore,F., Zambrano,N., Minopoli,G., Donini,V., Duilio,A. and Russo,T. (1995) The regions of the Fe65 protein homologous to the phosphotyrosine interaction/phosphotyrosine binding domain of Shc bind the intracellular domain of the Alzheimer's amyloid precursor protein. *J. Biol. Chem.*, **270**, 30853–30856.

Haass,C., Hung,A.Y., Schlossmacher,M.G., TeplowD.B. and Selkoe,D.J. (1993) beta-Amyloid peptide and a 3-kDa fragment are derived by distinct cellular mechanisms. *J. Biol. Chem.*, **268**, 3021–3024.

Harrison,S.C. (1996) Peptide-surface association: the case of PDZ and PTB domains. *Cell*, **86**, 341–343.

Hendrickson,W.A. (1991) Determination of macromolecular structures from anomalous diffraction of synchrotron data. *Science*, **254**, 51–58.

Hendrickson,W.A., Horton,J.R. and LeMaster,D.M. (1990) Seleno-methionyl proteins produced for analysis by multiwavelength anomalous diffraction (MAD): a vehicle for direct determination of three-dimensional structure. *EMBO J.*, **9**, 1665–1672.

Honig,B. and Nicholls,A. (1995) Classical electrostatics in biology and chemistry. *Science,* **268**, 1144–1149.

Isakoff,S.J. *et al.* (1996) Interaction between the phosphotyrosine binding domain of Shc and the insulin receptor is required for Shc phosphorylation by insulin *in vivo*. *J. Biol. Chem.*, **271**, 3959–3962.

Jones,T.A., Zou,J.Y., Cowan,S.W. and Kjeldgaard,M. (1991) Improved methods for building protein models in electron density maps and the location of errors in these models. *Acta Crystallogr.*, **A47**, 110–119.

Kavanaugh,W.M. and Williams,L.T. (1994) An alternative to SH2 domains for binding tyrosine-phosphorylated proteins. *Science,* **266**, 1862–1865.

Kavanaugh,W.M., Turck,C.W. and Williams,L.T. (1995) PTB domain binding to signaling proteins through a sequence motif containing phosphotyrosine. *Science*, **268**, 1177–1179.

Koo,E.H. and Squazzo,S.L. (1994) Evidence that production and release of amyloid β-protein involves the endocytic pathway. *J. Biol. Chem.*, **269**, 17386–17389.

Kraulis,P. (1991) MOLSCRIPT: a program to produce both detailed and schematic plots of protein structures. *J. Appl. Crystallogr.*, **24**, 946–950.

Kuriyan,J. and Cowburn,D. (1997) Modular peptide recognition domains in eukaryotic signaling. *Annu. Rev. Biophys. Biomol. Struct.*, **26**, 257–286.

Ladbury,J.E., Lemmon,M.A., Zhou,M., Green,J., Botfield,M.C., and Schlessinger,J. (1995) Measurement of the binding of tyrosyl phosphopeptide to SH2 domains: a reappraisal. *Proc. Natl Acad. Sci. USA*, **92**, 3199–3203.

Lai,A., Sisodia,S.S. and Trowbridge,I.S. (1995) Characterization of sorting signals in the beta-amyloid precursor protein cytoplasmic domain. *J. Biol. Chem.*, **270**, 3565–3573.

Laminet,A.A., Apell,G., Conroy,L. and Kavanaugh,W.M. (1996) Affinity, specificity, and kinetics of the interaction of the SHC phosphotyrosine binding domain with asparagine-X-X-phosphotyrosine motifs of growth factor receptors. *J. Biol. Chem.*, **271**, 264–269.

Lee,C.H., Kominos,D., Jacques,S., Margolis,B., Schlessinger,J., Shoelson,S.E. and Kuriyan,J. (1994) Crystal structures of peptide complexes of the amino-terminal SH2 domain of the Syp tyrosine phosphatase. *Structure*, **2**, 423–438.

Lemmon,M.A., Ferguson,K.M. and Schlessinger,J. (1996) PH domains: diverse sequences with a common fold recruit signaling molecules to the cell surface. *Cell*, **85**, 621–624.

Macias,M.J., Musacchio,A., Ponstingl,H., Nilges,M., Saraste,M. and Oschkinat,H. (1994) Structure of the pleckstrin homology domain from beta-spectrin. *Nature*, **369**, 675–677.

Mandiyan,V., O'Brien,R., Zhou,M., Margolis,B., Lemmon,M.A., Sturtevant,J.M. and Schlessinger,J. (1996) Thermodynamic studies of SHC phosphotyrosine interaction domain recognition of the NPXpY motif. *J. Biol. Chem.*, **271**, 4770–4775.

McLoughlin,D.M. and Miller,C.C.J. (1996) The intracellular cytoplasmic domain of the Alzheimer's disease amyloid precursor protein interacts with phosphotyrosine-binding domain proteins in the yeast two-hybrid system. *FEBS Lett*., **397**, 197–200.

Milia,E., Di Somma,M.M., Baldoni,F., Chiari,R., Lanfrancone,L., Pelicci,P.G., Telford,J.L. and Baldari,C.T. (1996) The aminoterminal phosphotyrosine binding domain of Shc associates with ZAP-70 and mediates TCR dependent gene activation. *Oncogene*, **13**, 767–775.

Muller,U., Cristina,N., Li,Z.W., Wolfer,D.P., Lipp,H.P., Rulicke,T., Brandner,S., Aguzzi,A. and Weissmann,C. (1994) Behavioral and anatomical deficits in mice homozygous for a modified beta-amyloid precursor protein gene. *Cell,* **79**, 755–765.

Nicholls,A., Sharp,K.A., and Honig,B. (1991) Protein folding and association: insights from the interfacial and thermodynamic properties of hydrocarbons. *Proteins*: *Struct. Funct. Genet.*, **11**, 281–296.

O'Bryan,J.P., Songyang,Z., Cantley,L., Der,C.J. and Pawson,T. (1996) A mammalian adaptor protein with conserved Src homology 2 and phosphotyrosine-binding domains is related to Shc and is specifically expressed in the brain. *Proc. Natl Acad. Sci. USA*, **93**, 2729–2734.

Panayotou,G., Gish,G., End,P., Truong,O., Gout,I., Dhand,R., Fry,M.J., Hiles,I., Pawson,T. and Waterfield,M.D. (1993) Interactions between SH2 domains and tyrosine phosphorylated platelet-derived growth factor beta-receptor sequences: analysis of kinetic parameters by a novel biosensor-based approach. *Mol. Cell. Biol.*, **13**, 3567–3576.

Pelicci,G. *et al.* (1996) A family of Shc related proteins with conserved PTB, CH1 and SH2 regions. *Oncogene*, **13**, 633–641.

Pratt,J.C., Weiss,M., Sieff,C.A., Shoelson,S.E., Burakoff,S.J. and Ravichandran,K.S. (1996) Evidence for a physical association between the Shc-PTB domain and the beta c chain of the granulocyte-macrophage colony-stimulating factor receptor. *J. Biol. Chem.*, **271**, 12137–12140.

Ravichandran,K.S., Igras,V., Shoelson,S.E., Fesik,S.W. and Burakoff,S.J. (1996) Evidence for a role for the phosphotyrosine-binding domain of Shc in interleukin 2 signaling. *Proc. Natl Acad. Sci. USA*, **93**, 5275–5280.

Sawka-Verhelle,D., Tartare-Deckert,S., White,M.F. and Van Obberghen,E. (1996) Insulin receptor substrate-2 binds to the insulin receptor through its phosphotyrosine-binding domain and through a newly identified domain comprising amino acids 591–786. *J. Biol. Chem.*, **271**, 5980–5983.

Sheldrick,G. (1991) *Heavy Atom Location using SHELXS-90.* Daresbury CCP4 Meeting (Patterson interpretation and the use of macromolecular delta-F data).

Songyang,Z. *et al.* (1993) SH2 domains recognize specific phospho-peptide sequences. *Cell*, **72**, 767–778.

Trub,T., Choi,W.E., Wolf,G., Ottinger,E., Chen,Y., Weiss,M. and Shoelson,S.E. (1995) Specificity of the PTB domain of Shc for beta turn-forming pentapeptide motifs amino-terminal to phosphotyrosine. *J. Biol. Chem.*, **270**, 18205–18208.

van der Geer,P., Wiley,S., Gish,G.D., Lai,V.K., Stephens,R., White,M.F., Kaplan,D. and Pawson,T. (1996) Identification of residues that control specific binding of the Shc phosphotyrosine-binding domain to phosphotyrosine sites. *Proc. Natl Acad. Sci. USA*, **93**, 963–968.

Waksman,G., Shoelson,S.E., Pant,N., Cowburn,D. and Kuriyan,J. (1993) Binding of a high affinity phosphotyrosyl peptide to the Src SH2 domain: crystal structures of the complexed and peptide-free forms. *Cell,* **72**, 779–790.

White,M.F. (1996) The IRS-signalling system in insulin and cytokine action. *Philos. Trans. R. Soc. Lond. Ser. B*, **351**, 181–189.

Wolf,G., Trub,T., Ottinger,E., Groninga,L., Lynch,A., White,M.F., Miyazaki,M., Lee,J. and Shoelson,S.E. (1995) PTB domains of IRS-1 and Shc have distinct but overlapping binding specificities. *J. Biol. Chem.*, **270**, 27407–27410.

Zhang,K.Y.J. and Main,P. (1990) The use of Sayre's equation with solvent flattening and histogram matching for phase extension and refinement of protein structures. *Acta Crystallogr.*, **A46**, 377–381.

Zhou,M.M., Harlan,J.E., Wade,W.S., Crosby,S., Ravichandran,K.S., Burakoff,S.J. and Fesik,S.W. (1995a) Binding affinities of tyrosine-phosphorylated peptides to the COOH-terminal SH2 and NH2-terminal phosphotyrosine binding domains of Shc. *J. Biol. Chem.*, **270**, 31119–31123.

Zhou,M.M., Ravichandran,K.S., Olejniczak,E.F., Petros,A.M., Meadows,R.P., Sattler,M., Harlan,J.E., Wade,W.S., Burakoff,S.J. and Fesik,S.W. (1995b) Structure and ligand recognition of the phosphotyrosine binding domain of Shc. *Nature*, **378**, 584–592.

Zhou,S., Margolis,B., Chaudhuri,M., Shoelson,S.E. and Cantley,L.C. (1995c) The phosphotyrosine interaction domain of SHC recognizes tyrosine-phosphorylated NPXY motif. *J. Biol. Chem.*, **270**, 14863–14866.

Zhou,M.M., Huang,B., Olejniczak,E.T., Weadows,R.P., Shuker,S.B., Miyazaki,M., Trub,T., Shoelson,S.E. and Felsik,S.W. (1996) Structural basis for IL-4 receptor phosphopeptide recognition by the IRS-1 PTB domain. *Nature Struct. Biol.*, **3**, 388–393.